Intestinal CD4-CD8αβ-TCRαβ+ T cells function as tolerogenic antigen presenting cells

Yasuhiro Nemoto (ynemoto.gast@tmd.ac.jp)
Tokyo Medical and Dental University

Shohei Tanaka
Tokyo Medical and Dental University

Yuria Takei
Tokyo Medical and Dental University

Ryo Morikawa
Tokyo Medical and Dental University

Shigeru Oshima
Tokyo Medical and Dental University https://orcid.org/0000-0003-1186-9177

Takashi Nagaishi
Tokyo Medical and Dental University

Kiichiro Tsuchiya
Tokyo Medical and Dental University

Tetsuya Nakamura
Juntendo University https://orcid.org/0000-0002-4244-9119

Kento Takenaka
Tokyo Medical and Dental University

Kazuo Ohtsuka
Tokyo Medical and Dental University

Xigui Chen
Tokyo Medical and Dental University

Hitoshi Okazawa
Tokyo Medical and Dental University

Ryuichi Okamoto
Tokyo Medical and Dental University https://orcid.org/0000-0002-7047-571X

Mamoru Watanabe
Tokyo Medical & Dental University

Ulrich von Andrian
Harvard Medical School https://orcid.org/0000-0003-4231-2283

Research Article

Keywords: intestinal immune system, antigens, murine DNT cells

Posted Date: August 24th, 2020

DOI: https://doi.org/10.21203/rs.3.rs-60691/v1

Intestinal CD4$^-$CD8αβ$^-$TCRαβ$^+$ T cells function as tolerogenic antigen presenting cells

Alternative Title: Intestinal CD8αβ$^-$TCRαβ$^+$T cells induce tolerance to intestinal antigens

*Yasuhiro Nemoto[1,2,7], Shohei Tanaka[1], Yuria Takei[1], Ryo Morikawa[1], Shigeru Oshima[1], Takashi Nagaishi[1,2], Kiichiro Tsuchiya[1], Tetsuya Nakamura[1,6], Kento Takenaka[1], Kazuo Ohtsuka[1], Xigui Chen[4], Hitoshi Okazawa[4], Ryuichi Okamoto[1,3], Mamoru Watanabe[1,5] and Ulrich H.von Andrian[7,8]

[1]Department of Gastroenterology and Hepatology, Graduate School, Tokyo Medical and Dental University (TMDU), Tokyo, Japan. [2]Department of Advanced Therapeutics for GI Diseases, TMDU, Tokyo, Japan. [3]Center for Stem Cell and Regenerative Medicine, TMDU, Tokyo, Japan. [4]Department of Neuropathology, medical research institute, TMDU, Tokyo, Japan. [5]Advanced Research Institute, TMDU. [6]Department of Research and Development for Organoids Juntendo University School of Medicine, [7]Department of Immunology, Harvard Medical School, Boston, USA. [8]Ragon Institute of MGH, MIT and Harvard, Cambridge, MA.

The intestinal immune system is constantly exposed to a plethora of antigens (Ags) from innocuous ingested material and the commensal flora that must be distinguished from pathogen-derived antigens. To this end, a number of anatomic, cellular and molecular mechanisms operate in the intestinal tract to acquire, process, present and interpret Ags from the intestinal lumen. The intestinal mucosa is also populated by a large number of T cells that reside within the epithelial lining (intraepithelial lymphocytes, IELs), in the underlying lamina propria (LPLs) and in gut-associated lymphoid tissues (GALT). Both IELs and LPLs are heterogeneous populations consisting of conventional CD4$^+$ and CD8$^+$ T cells and numerous unconventional T cells, including TCRγδ$^+$ T cells and CD4$^-$CD8αβ$^-$TCRαβ$^+$T cells (double negative; DNT cells). The latter are rarely found in non-intestinal tissues and their function is still enigmatic. Here, we show that murine DNT cells in the small intestine (SI) reach across the epithelial barrier to capture luminal Ags. A sizeable fraction of DNT cells in

Peyer's patches (PPs), mesenteric lymph nodes (MLNs) and among LPLs, but not among IELs, express MHC-II, but little or no classical co-stimulatory molecules, suggesting that DNT cells-mediated Ag presentation to naïve $CD4^+$ T cells may trigger tolerogenic rather than effector responses. Indeed, intestinal DNT cells, particularly in PPs, acquire, process and present antigenic proteins and tolerize Ag-specific $CD4^+$ T cells. Conditional genetic ablation of MHC-II in T cells disabled this suppressive function and rendered mutant mice hypersusceptible to DSS colitis. Moreover, similar to our findings in mice, DNT cells in human SI express HLA-DR and readily uptake exogenous Ags. Intriguingly, intestinal DNT cells in Crohn's disease patients expressed lower levels of HLA-DR than control patients. These findings suggest that MHC-II^+ DNT cells play a key role in intestinal immune homeostasis and may contribute to the pathogenesis of inflammatory bowel disease.

The intestinal tract has a highly specialized immune landscape, which must simultaneously maintain tolerance to food Ags and commensals and mount appropriate and effective immune responses against enteric pathogens. To distinguish harmful from harmless Ags, the intestinal mucosa features several specialized cell subsets to sample Ags. These include M cells in PPs, which take up luminal material and deliver it to dendritic cells (DCs)[1-3]. CX_3CR1^+ macrophages extend trans-epithelial dendrites, which can penetrate tight junctions and capture luminal Ags[4, 5], as well as goblet cells that enable the passage of luminal molecules across the mucosal barrier for acquisition by $CD103^+$ DCs[6]. Interestingly, different Ag uptake pathways are thought to promote different immunological outcomes[7]. For example, M cells are implicated in the induction of IgA-producing plasma cells[8], while goblet cells are involved in oral tolerance[6]. In addition,, certain subsets of innate lymphoid lineage cells (ILCs) are also involved in Ag uptake and presentation in the intestine. For example, a population of LPLs that express CD8α homodimers ($CD8\alpha\alpha^+CD3^-$ ILCs) possess Ag processing and presentation capacity and have been implicated in the pathogenesis of necrotizing enterocolitis[9]. Similarly, ILC3 in MLNs express MHC-II and are thought to induce tolerance of $CD4^+$ T cells that recognize microbiota-

derived Ags[10].

In addition to these ILC subsets, the intestinal tract harbors abundant unconventional T cell (i.e. $CD3^+$) subsets, including $TCR\gamma\delta^+$ T cells and $CD4^-CD8\alpha\beta^-TCR\alpha\beta^+$T cells (DNT cells)[11-13]. These T cells are plentiful among intestinal IELs and LPLs, but they are much less frequent in most other tissues. Intestinal γδ and DNT cells differ from conventional $CD4^+$ and $CD8^+$ T cells in many aspects. Most, but not all, express the CD8αα homodimer and their TCRs are thought to recognize self-Ags. Phenotypically, these cells often express various NK receptors, but they do not express many common markers of conventional T cells[11]. Unlike conventional intestinal $CD4^+$ and $CD8^+$ T cells, which are absent at birth and increase with age, intestinal γδ and DNT cells are abundant at birth and decrease with age. These cells are thought to exert anti-inflammatory effects rather than promoting intestinal immunity and inflammation, but the mechanisms by which they exert their functions remain to be clarified[11-12].

Here, we hypothesized that intestinal γδ and/or DNT cells may function as tolerogenic Ag presenting cells (APCs). This idea seemed particularly attractive for γδ T cells, which are abundant in the intraepithelial compartment from where they can dynamically move to the lamina propria[14]. Indeed, human peripheral blood γδ T cells have been shown to function as APCs[15, 16], and murine γδ T cells express modest amounts of MHC-II mRNA, although their role in Ag presentation has been unclear[17].

To systematically address whether and which murine intestinal T cell subsets may have the potential to function as APCs, we measured MHC-II expression. To this end, we performed flow cytometry on $CD3^+$ T cells from different compartments in the SI, PPs, MLNs and spleen by gating on four discrete subsets: (1) $TCR\gamma\delta^+$ (γδ); (2) $TCR\alpha\beta^+CD4^+CD8\alpha\beta^-$ (CD4); (3) $TCR\alpha\beta^+CD4^-CD8\alpha\beta^+$ (CD8); and (4) $TCR\alpha\beta^+CD4^-CD8\alpha\beta^-$ (DN) (**Fig. 1a**). Consistent with previous reports[11, 12], the γδ and DN subsets represented 40-50% of T cells among IELs and LPLs in SI and were less frequent in PPs, MLNs and spleen (**Sup. Fig. 1**).

The frequency and composition of intestinal MHC-II$^+$ cells among both the CD3$^-$ non-T and CD3$^+$ T cell subset varied with the animals' age (**Fig. 1b,c, Sup. Fig. 2**). In juvenile mice (6 weeks old), the abundance of MHC-II$^+$ T cells in IELs and LPLs was low (<5%) regardless of subset, but by 10 weeks this frequency had increased significantly, especially for DNT cells among which 9.5 ± 1.9% and 17.5 ± 3.2% expressed MHC-II among IELs and LPLs, respectively. The positive correlation between age and frequency of MHC-II$^+$ DNT cells among SI LPLs continued well beyond 10 weeks and was statistically highly significant (**Fig. 1c**). Similar frequencies of MHC-II$^+$ γδ and DNT cells were also seen in colon LPLs (**Sup. Fig. 3**). MHC-II was even more prominently expressed on DNT cells in PPs where as many as 38.7% and 56.4% were positive by 6 and 10 weeks, respectively (**Fig. 1d, Sup. Fig. 2**). PPs also harbored MHC-II$^+$ cells among the γδT > CD4 > CD8 subsets, but at markedly lower frequencies than among DNT cells.

As expected, most γδ and DNT cells in the SI expressed CD8αα (i.e. they were CD8α$^+$CD8β$^-$) while ~half in PPs and less than 20% in MLNs and spleen had this phenotype (**Sup. Fig. 4a**). Interestingly, among DNT cells in PPs, MHC-II was preferentially expressed in the CD8α$^-$ subset (**Sup. Fig. 4b**). Moreover, intestinal T cells (esp. DNT cells) in MHC-II-eGFP reporter mice expressed GFP with similar frequencies and tissue distribution as observed by immuno-fluorescence (**Sup. Fig. 5**), indicating that the apparent MHC-II signal was not due to non-specific staining or cross-reactivity of our monoclonal antibody.

In light of the fact that DNT cells contained the highest frequency of MHC-II$^+$ cells among all intestinal T cells, especially in PPs, we focused our further analysis on DNT cells whose function is still largely enigmatic. DNT cells display an unusual pattern of MHC restriction that is non-overlapping with that of conventional CD4$^+$ or CD8αβ$^+$ T cells[18] . Moreover, DNT cells are thought to play a protective role in the pathogenesis of colitis, but the mechanism remains to be clarified[19 20]. Indeed, when compared to CD11c$^+$ DCs, most MHC-II$^+$ PP DNT cells expressed little or no costimulatory molecules, such as CD40, CD80 and CD86, suggesting that DNT-mediated Ag presentation may result in tolerogenic rather than effector

responses by T cells (**Fig. 1e** and **Sup. Fig. 6**).

To further explore the biology and function of DNT cells and to compare them to other intestinal T cells, we performed a transcriptome analysis of each T cell subset in PPs. Consistent with our flow cytometry results, DN and γδ T cells, but not CD4 or CD8 T cells, expressed high mRNA levels for MHC-II and related molecules (**Fig. 1f**). DN and γδ T cells in PPs also expressed many NK markers and granzymes A and B (**Sup. Fig. 7**), which is consistent with previous reports of expression profiles of DN and γδ T cells in IEL[11, 12]. DNT cells were transcriptionally more similar to γδ T cells than to CD4 or CD8 T cells, but DNT cells were distinct from γδ T cells by expressing higher levels of several genes, including *Klra15, Pabpc4, Myl1, Klra6, Klra5, Reg3b and trf* (**Sup. Fig. 8**). Principle component (PCA) analysis and Volcano Plots also show the similarity of DNT cells and γδ T cells and difference from CD4 or CD8 T cells, which is consistent with the previous report about natural IELs (γδ and DN) and induce IELs (CD4 and CD8)[11, 12]**(Sup. Fig. 9, 10)**.

At the protein level, most MHC-II$^+$ DNT cells in the intestine and, in particular, in PPs (but not in MLN or spleen) expressed high levels of EpCAM, an adhesion molecule that is also expressed on intestinal epithelial cells (IECs) and mediates interactions between IECs and IELs[21] (**Sup. Fig. 11a-c**). By contrast, conventional T cells in PPs expressed little or no EpCAM. γδ and DNT cells were also distinct from intestinal CD4 and CD8 T cells on a functional level. They produced little IFN-γ or IL-17A upon activation unlike most conventional T cells and mucosa-associated invariant T (MAIT) cells[22], which function primarily by orchestrating cytokine dependent effector responses to infectious pathogens (**Sup. Fig. 12**).

In light of these observations, we asked whether DNT cells possess the capacity to acquire and process exogenous Ags. To this end, T cell subsets in SI and, as a positive control, CD11c$^+$ myeloid cells in MLN were purified and incubated with DQ-Ovalbumin (DQ-OVA), a fluorescently tagged protein that becomes brightly fluorescent upon endocytosis and intracellular proteolysis[10]. Remarkably, DNT cells acquired and processed a large amount of DQ-OVA, exceeding even

CD11c$^+$ cells (**Fig. 1g**). γδ T cells, but not CD4 or CD8 T cells, also showed a modest uptake. On the other hand, when isolated cells were incubated with labeled bacteria only CD11c$^+$ cells acquired fluorescent material, indicating that DNTs acquire Ags via macropinocytosis or other endocytosis pathways, rather than phagocytosis (**Sup. Fig. 13**).

Next, we asked whether DNT cells can also acquire soluble macromolecules *in vivo*. For this, Dextran-Alexa Fluor488 (Dex-AF488) was injected into the ligated small intestine and cellular dextran uptake was assessed 5h later. Indeed, DNT cells, but no other T cell subset, in IELs, LPLs and PPs accumulated Dex-AF488 (**Fig. 2a**). Negligible numbers of Dex-AF488$^+$ cells were found in MLNs and spleen at this time point (data not shown), indicating that the cells that had acquired fluorescent material in the gut lumen remained, at least initially, confined to the intestine.

To test more rigorously whether DNT cells traffic after Ag uptake from the gut to MLNs, we used *Kaede* transgenic mice, which express a photoconvertible fluorescent protein[23]. The serosal side of the small intestine of *Kaede* mice was illuminated with a blue laser and 48h later, photo-converted T cells in each intestinal compartment were enumerated by flow cytometry. There were comparable numbers of photo-converted γδ, DNT cells and TCR$^-$ leukocytes in MLNs, while almost no photo-converted CD4 or CD8 T cells were detected (**Fig. 2b,c**).

In aggregate, the above results indicate that many intestinal DNT cells express MHC-II and acquire soluble material from the intestinal lumen, which they can then carry to MLN. Thus, we asked whether DNT cells can present exogenous Ags to CD4 T cells. To this end, T cell subsets were purified from PPs and co-cultured with OVA and CFSE-labeled naive OT-II-CD4 T cells. On day 5, 6 and 8, the recovered number and CFSE fluorescence of OT-II cells were analyzed. Indeed, DNT cells and, to some degree, also γδ T cells, but not CD4 or CD8 T cells, induced OT-II cell proliferation (**Fig. 2d**). However, OT-II cells that were exposed to Ag presenting DNT cells produced only modest amounts of cytokine

and had undergone fewer divisions and expressed fewer phenotypic markers of activated effector cells when compared to OT-II cells that had been co-cultured with OVA pulsed CD11c^{+} DCs (**Fig. 2d-g** and **Sup. Figs. 14, 15**). These results are consistent with the idea that incomplete Ag presentation (i.e. TCR stimulation with little or no co-stimulation) by γδ and DNT cells may have induced an anergic state in responsive T cells. Indeed, the number of viable OTII-CD4 T cells co-cultured with γδ or DNT cells was dramatically reduced on day 6 and 8 (**Fig. 2e-f**). Similar to PPs, γδ and DNT cells harvested from MLNs also had the capacity for Ag presentation, whereas IELs and LPLs were inactive (**Sup. Fig. 16a-c**), presumably due to the low expression of MHC-II in this compartment (**Fig. 1d**).

Next we sought to clarify the physiological importance of DNT cells mediated uptake of intestinal Ag *in vivo*. Thus, we performed and *ex vivo* Ag presentation experiments[6, 24] by feeding mice with a diet containing 1% OVA for 3 days and then coculturing sorted γδ, DN, CD4, CD8 and TCRβ^{-}TCRγδ^{-} cells from PPs and CD11c^{+} cells from MLN with CFSE-labeled naïve OT-II CD4 T cells. In these experiments, the percentage and number of divided OT-II cells in co-cultures with DNT cells was higher than in any other coculture setting **(Fig. 2h-j,)**.

Having determined that certain unconventional intestinal T cells, most prominently the DNT cells subset, can acquire antigenic material from the gut lumen and then process and present this material to cognate naive CD4 T cells, we set out to assess the patho-physiological significance of these observations. To this end, we crossed CD4-Cre^{+} mice[25] with H2-Ab1$^{flox/flox}$ mice[10] to conditionally delete MHC-II in T cells. In these animals, expression of MHC-II on intestinal ILC3 and CD3^{-} cells remained unchanged. Although MHC-II expression on DNT cells was not completely deleted in CD4-Cre^{+}xH2-Ab1$^{flox/flox}$ mice, it was significantly reduced compared to littermate (**Sup. Fig. 17a-d**). The number of Tregs in CD4-Cre^{+}xH2-Ab1$^{flox/flox}$ mice remained unchanged when compared to wildtype (**Sup. Fig. 17e**).

Next, we set out to compare the ability of DNT cells from conditional mutant donors and WT littermates to elicit a tolerogenic response in naive T cells . To

this end, naive OT-II CD4 T cells co-cultured with purified γδ, DN, CD4 or CD8 T cells from PP in the presence of antigenic peptide ($OVA_{323-339}$). Two hours later, MLN $CD11c^+$ cells were added to the cultures. In the presence of fully MHC-II sufficient DNT cells significantly fewer OT-II cells were recovered than in co-cultures with any other intestinal cell subset, whereas conditional deletion of MHC-II in T cells abrogated this apparent tolerogenic effect of DNT cells **(Fig. 2k and Sup. Fig. 18a-c).**

Next, we set out to directly observe intestinal T cells *in situ* using multi-photon intravital microscopy (MP-IVM) in anesthetized mice. As shown in **Fig. 3a** and **Sup. Movie 1**, T cells in DPE-GFP mice, in which T cells express GFP[26], numerous GFP^+ cells moved dynamically between the LP and the intra-epithelial region. GFP^+ T cells in Tcrd-GFP mice showed a similar behavior (**Fig. 3b** and **Sup. Movie 2**), consistent with a previous report[14]. Since some non-T cells, such as plasmacytoid dendritic cells (pDC) and some macrophages, are known to express GFP in DPE-GFP mice [27, 28], we also performed MP-IVM in the SI of DPE-GFPxRAG-$1^{-/-}$ mice. As shown in **Fig. 3c** and **Sup. Movie 3**, the motility of the sparse GFP^+ non-T cells in these mice was low, and they rarely localized to the intra-epithelial region. Although some GFP^+ cells in CX_3CR1-GFPmice were in contact with IEC, most of them located in LP lesion (**Fig. 3d** and **Sup. Movie 4**). The average speed of GFP^+ cells in DPE-GFP and Tcrd-GFP mice was higher than those of DPE-GFPxRAG-$1^{-/-}$ or CX_3CR1-GFP, but there was no difference in the track length between DPE-GFP/Tcrd-GFP and CX_3CR-1GFP mice (**Fig. 3e, f)**. The number of GFP^+ cells that were positioned in the intra-epithelial compartment and/or were exposed to the intestinal lumen was higher in DPE-GFP and Tcrd-GFP mice than in DPE-GFP x $RAG^{-/-}$ or CX_3CR1-GFP mice (**Fig. 3g, h**). Some GFP^+ cells in DPE mice were observed to extend protrusions across the epithelial layer (**Fig. 3i** and **Sup. Movie 5**), a phenomenon that was not observed in Tcrd-GFP or DPE-GFPxRAG$1^{-/-}$ mice. Transepithelial protrusions of GFP^+ cells, presumably reflecting macrophages, were also occasionally detected in CX_3CR1-GFP mice, consistent with previous studies[4, 5], but the frequency of these occurrences was much lower than in DPE-GFP mice. When DPE-GFP

mice were injected with OVA-AF594 into the lumen of the small intestine, GFP$^+$ (presumably DNT) cells could be seen ~3h later that had acquired the fluorescent Ag in the lumen and then moved it across the epithelial barrier (**Fig. 3j** and **Sup. Movie 6**).

To more rigorously compare each T cell subset *in vivo*, we resorted to an adoptive transfer strategy. Purified γδ, DNT, CD4 or CD8-IELs from EGFP-Tg mice were separately transferred into individual NOD.scid.IL-2Rγ$^{-/-}$ (NSG) mice. Seven to eight weeks later, intravital imaging was performed in the small intestine. We confirmed more than 95% purity before the transfer. We also performed FACS analysis after the intravital imaging and confirmed that each subset did not change even 7-8 weeks after the transfer (**Sup. Fig 19a-b**).
These experiments revealed distinct differences in the distribution and motility of each transferred T cell subset **(Fig. 3k-n** and **Sup. Movie7-10).** For example, CD4 T cells migrated somewhat more slowly and with shorter track length than other T cells **(Fig. 3o, p)**. Some cells in the LP lesion of CD4→NSG mice did not move **(Fig. 3m** and **Sup. Movie9)**. The track length of DNT cells was the shortest, even **(Fig. 3o, p)**, which suggests that the movement of DNT cells was restricted. Of note, GFP$^+$ cells in DN→NSG mice were frequently observed to attached to IECs and lumen **(Fig. 3l, q, r** and **Sup. Movie8)**. As shown in **Supplemental movie 11**, multiple GFP$^+$ cells in recipients of DNT cells meandered between the LP and IE compartment and extended dendrites toward the intestinal lumen, a behavior that was not seen in DPE-GFP mice.
Having characterized intestinal MHC-II$^+$ T cells, particularly the DNT cells subset, at steady-state, we set out to assess their role in intestinal inflammation using CD4-Cre$^+$ x H2-Ab1$^{flox/flox}$ mice. In our animal colony, CD4-Cre$^+$ x H2-Ab1$^{flox/flox}$ mice did not develop spontaneous colitis, however, upon challenge with 3% DSS for 5 days the mutant mice developed much more severe colitis than WT littermates, as evidenced by accelerated loss of body weight, shortening of the colon and clinical score (**Fig. 4a-d**). Accordingly, histologic evaluation of colons revealed a much more pronounced trans-mural inflammation in CD4-Cre$^+$ x H2-Ab1$^{flox/flox}$ mice (**Fig. 4e-f**).

In aggregate, the above experiments in murine models indicate that many unconventional intestinal T cells, most notably the DNT cells subset, express MHC-II and have the capacity to acquire and present soluble antigenic material both *in vitro* and *in vivo*. Intravital imaging experiments suggest that DNT cells are highly motile and rapidly shuttle between the LP and the IE compartment from where they may directly access Ag in the intestinal lumen by extending transepithelial processes. However, DNT cells are distinct from the majority of T cell subsets among IEL, which are a tissue resident population[11-13], whereas DNT cells can exit the gut and migrate to MLN. In addition, a sizeable population of MHC-II$^+$ DNT cells also resides in PPs. When isolated from PPs, DNT cells as well as γδ T cells could present Ag to naive CD4 T cells, which resulted in anergy rather than effector activity, presumably because DNT cells do not express co-stimulatory molecules. Indeed, the presence of DNT cells suppressed in an MHC-II dependent manner the proliferation of CD4 T cells that were simultaneously exposed to Ag presenting CD11c$^+$ cells. Physiological relevance of these findings is implied by the observation that the conditional deletion of MHC-II in T cells markedly exacerbated DSS colitis, which is consistent with the idea that DNT cells function as tolerogenic APCs.

Finally, we asked whether these findings have a correlate in humans, particularly in the context of inflammatory bowel disease (IBD). To this end, biopsy samples of SI mucosa from patients with either Crohn's disease (CD) or other, non-inflammatory bowel diseases (non-IBD) were collected after obtaining informed consent (**Sup. Table 1-2**) and mononuclear cells were analyzed by flow cytometry.

Although the frequency of γδ and DNT cells was generally lower in humans than in mice, both subsets were readily detectable in both SI-IEL and LPL (**Fig. 4g**). In non-IBD samples, most (~55%-75%) human T cells expressed MHC-II regardless of subset, which is in contrast to intestinal T cells in mice where MHC-II was only found on γδ and DNT cells (**Fig. 4h**). However, similar to our findings in mice, only human DN and γδ T cells, but not CD4 or CD8 T cells in SI-LP took up OVA-DQ **(Figure 4i).**

Interestingly, in intestines of CD patients the expression of HLA-DR and antigen uptake ability of DN and γδ T cells were significantly reduced as compared to non-IBD patients **(Figure 4h, i)**. There was no statistically significant difference between the ages of patients CD (38.5±4.78 years) and non-IBD patients (52.4±6.59 years), however, our CD patients cohort included more male (8) and fewer female (3) patients than our non-IBD control group (6 male and 5 female). However, as shown in **supplemental figure 20**, there was no difference between male and female control patients in the expression of HLA-DR on LP DNTs. Interestingly, the expression of HLA-DR on DNTs in active CD patients was higher than in patients in remission (**Sup. Fig. 21**), suggesting that the low expression of HLA-DR on DNTs in CD patients is not due to inflammation.

γδ and DNT cells are uniquely abundant in the intestine, but rare in other organs. Although they differ from conventional CD4 or CD8 T cells in many aspects, their function is not completely clear. Results of *in vivo* experiment using knockout mice (*Tcrd*$^{-/-}$) or reporter mice (*Tcrd*-eGFP) suggest that γδ T cells combine features of adaptive and innate immune cells[11-13, 17]. However, much less information is available on DNT cells, which have remained largely enigmatic. We now show that both human and murine intestinal DNT cells express MHC-II and have the ability to uptake, process and present soluble Ags resulting in an anergic response by naïve CD4 T cells.

In some previous papers, this subset was sometimes called as CD8αα^{+} T cells[29, 30], because most of them express CD8αα homodimer. In the current study, we defined CD3^{+}CD4^{-}CD8β^{-}TCRαβ^{+} T cells as DNT cells, because considerable part of them outside the intestine doesn't express CD8αα (**Sup. Fig. 4**). In addition, some papers suggest that CD8αα can be transiently expressed[31, 32], so it is possible that the CD8αα cells are in constant exchange with the CD8αα-neg subset. That's why we selected "DNT cells" in ref 11 and 12 as more stable and reliable definition.

In some papers, CD4^{-}CD8α^{-}TCRαβ^{+} T cells are defined as DNT cells[33]. This fraction is not same as DNT cells in the current study, because considerable part

of DNTs expresses CD8αα.

Our findings shed new light on previous studies on the role of unconventional T cells in IBD. For example, DNT cells were shown to suppress colitis in RAG deficient recipients of adoptively transferred $CD4^+CD45RB^{high}$ T cells, but the mechanism has been unclear[19]. More recently, it was reported that Lck-Cre x $TAK1^{flox/flox}$ mice are nearly devoid of $CD8\alpha^+TCR\beta^+$IELs and develop $CD4^+$ T cell-dependent colitis[20] The idea that DNT cells promote immunologic tolerance by presenting intestinal Ags offers a potential mechanistic explanation for these observations.

Recently, it was reported that ILC3 cells also express MHC-II and induce anergy in $CD4^+$ T cells[10]. However, in our hands, ILC3 are quite rare in the small intestine, whereas DNTs are encountered at higher frequencies (more than 10 times in SI-LP and PP, 6 times in MLN, data not shown). DNT cells were distinct from ILC3 or other innate lymphoid cells that have previously reported to work as APCs, because they express CD3 and TCRαβ, but not IL-17 or RORγt.

In the current study, we proved that DNT-IEL protruded into the small intestinal lumen, efficiently take up luminal antigens and migrate to MLN. In the PP, DNT cells expressed substantial level of MHC class II and low level of CD40 or CD80. T cell specific deletion of MHC class II leads to exacerbation of DSS colitis, which suggests that this incomplete antigen presentation by MHC class II^+ DNT cells induces anergy of gut trophic $CD4^+$ T cells in the GALT (**Supplemental Figure 22**). Intriguingly, intestinal DNT cells in Crohn's disease patients expressed lower levels of HLA-DR and lower antigen uptake ability than control patients. These findings suggest that MHC-II^+ DNTs play a key role in intestinal immune homeostasis and may contribute to the pathogenesis of inflammatory bowel disease.

METHODS SUMMARY

Mouse strains used in this study are detailed in online version of Materials and Methods. For *in vitro* antigen uptake and process experiments, 1 x 10^5 of sort-

purified γδ, DN, CD4, CD8 IELs or $CD11c^+$ MLN cells from wild type (WT) C57BL/6 mice were co-incubated with or without 20μg/ml DQ-Ovalbumin (Thermo Fisher Scientific) in the condition of 37℃ and 5%CO_2 for five hours. For *in vivo* antigen uptake experiments, a small incision was made on the abdomen of anesthetized C57BL/6 mice, and then small intestine was exposed and ligated for 3cm long. 500μg of 10KDa Dextran-Alexa Flour 488 (Thermo Fisher Scientific) was injected into the ligated loop. Five hours later, mice were euthanized and analyzed by flow cytometer. For *in vitro* antigen presentation experiments, 1 x 10^4 of γδ, DN, CD4, CD8 PP cells or $CD11c^+$ MLN cells of C57BL/6 mice were co-incubated with or without 100μg of Ovalbumin (Low-endotoxin grade, Wako, Japan) and 1 x 10^5 of CFSE-labeled OTII $CD4^+CD44^-CD62L^+$ T cells in the condition of 37℃ and 5%CO_2 for 4 days. For *in vivo* Imaging experiments, mice were anesthetized and injected intravenously with Hoechst 33342 dye (Sigma Aldrich). A small incision was made on the abdomen and small intestine was exposed. Then mice were fixed on the customized stage and analyzed by the two-photon microscope. For DSS colitis model, $CD4Cre^+$ x H2-$Ab1^{fl/fl}$ mice and age matched, sex matched littermates in the same cage were assigned as each group. Then, 3% (w/v) DSS solution is administered as drinking water for 5 days. Mice were sacrificed and analyzed on day 9. For human experiments, adult patients in the hospital of TMDU from 2015 to 2019 with the informed consent were involved. Biopsy samples from ileum of CD or non-IBD patients were collected by colonoscopy or balloon assisted small bowel endoscopy and used for flow cytometry analysis or *in vitro* antigen uptake experiments. All animal studies were approved by the Institutional Animal Care and Use Committee of Harvard Medical School in U.S. and by the Institutional Animal Care and Use Committee of Tokyo Medical and Dental University in Japan, and complied with National Institutes of Health guidelines. All human studies were approved by the research ethics committee of Tokyo Medical and Dental University.

Online Content. Any additional Methods, data availability statement, supplemental reference, supplemental figures, tables and movies are available in the online version of the paper.

Reference

1. Neutra, M. R., Frey, A. & Kraehenbuhl, J. P. Epithelial M cells: gateways for mucosal infection and immunization. *Cell* **86**, 345-348 (1996).
2. Jang, M. H. *et al.* Intestinal villous M cells: an antigen entry site in the mucosal epithelium. *Proc. Natl. Acad. Sci. U S A* **101**, 6110-6115, doi:10.1073/pnas.0400969101 (2004).
3. Hase, K. *et al.* Uptake through glycoprotein 2 of FimH(+) bacteria by M cells initiates mucosal immune response. *Nature* **462**, 226-230, doi:10.1038/nature08529 (2009).
4. Rescigno, M. *et al.* Dendritic cells express tight junction proteins and penetrate gut epithelial monolayers to sample bacteria. *Nat. Immunol.* **2**, 361-367, doi:10.1038/86373 (2001).
5. Niess, J. H. *et al.* CX3CR1-mediated dendritic cell access to the intestinal lumen and bacterial clearance. *Science* **307**, 254-258, doi:10.1126/science.1102901 (2005).
6. McDole, J. R. *et al.* Goblet cells deliver luminal antigen to CD103+ dendritic cells in the small intestine. *Nature* **483**, 345-349, doi:10.1038/nature10863 (2012).
7. Knoop, K. A., Miller, M. J. & Newberry, R. D. Transepithelial antigen delivery in the small intestine: different paths, different outcomes. *Curr. Opin. Gastroenterol.* **29**, 112-118, doi:10.1097/MOG.0b013e32835cf1cd (2013).
8. Martinoli, C., Chiavelli, A. & Rescigno, M. Entry route of Salmonella typhimurium directs the type of induced immune response. *Immunity* **27**, 975-984, doi:10.1016/j.immuni.2007.10.011 (2007).
9. Van Kaer L**,** Algood HMS. *et al.* CD8αα^{+} innate-type lymphocytes in the intestinal epithelium mediate mucosal immunity. *Immunity* **41**, 451-464, doi: 10.1016/j.immuni.2014.08.010. Epub 2014 Sep 11. Erratum in: Immunity. 2014 Dec 18;41(6):1064 (2014).
10. Hepworth, M. R. *et al.* Innate lymphoid cells regulate CD4+ T-cell responses to intestinal commensal bacteria. *Nature* **498**, 113-117, doi:10.1038/nature12240 (2013).
11. Cheroutre, H., Lambolez, F. & Mucida, D. The light and dark sides of intestinal intraepithelial lymphocytes. *Nat. Rev. Immunol.* **11**, 445-456, doi:10.1038/nri3007 (2011).

12. Cheroutre, H. IELs: enforcing law and order in the court of the intestinal epithelium. *Immunol. Rev.* **206**, 114-131, doi:10.1111/j.0105-2896.2005.00284.x (2005).
13. Ishikawa, H. *et al.* Curriculum vitae of intestinal intraepithelial T cells: their developmental and behavioral characteristics. *Immunol. Rev.* **215**, 154-165, doi:10.1111/j.1600-065X.2006.00473.x (2007).
14. Edelblum, K. L. *et al.* Dynamic migration of γδ intraepithelial lymphocytes requires occludin. *Proc. Natl. Acad. Sci. U S A* **109**, 7097-7102, doi:10.1073/pnas.1112519109 (2012).
15. Brandes, M., Willimann, K. & Moser, B. Professional antigen-presentation function by human gammadelta T Cells. *Science* **309**, 264-268, doi:10.1126/science.1110267 (2005).
16. Moser, B. & Brandes, M. Gammadelta T cells: an alternative type of professional APC. *Trends Immunol.* **27**, 112-118, doi:10.1016/j.it.2006.01.002 (2006).
17. Vantourout, P. & Hayday, A. Six-of-the-best: unique contributions of γδ T cells to immunology. *Nat. Rev. Immunol.* **13**, 88-100, doi:10.1038/nri3384 (2013).
18. Mayans, S. *et al.* αβT cell receptors expressed by CD4(-)CD8αβ(-) intraepithelial T cells drive their fate into a unique lineage with unusual MHC reactivities. *Immunity* **41**, 207-218, doi:10.1016/j.immuni.2014.07.010 (2014).
19. Poussier, P., Ning, T., Banerjee, D. & Julius, M. A unique subset of self-specific intraintestinal T cells maintains gut integrity. *J. Exp. Med.* **195**, 1491-1497 (2002).
20. Sanjo, H., Tokumaru, S., Akira, S. & Taki, S. Conditional Deletion of TAK1 in T Cells Reveals a Pivotal Role of TCRαβ+ Intraepithelial Lymphocytes in Preventing Lymphopenia-Associated Colitis. *PLoS One* **10**, e0128761, doi:10.1371/journal.pone.0128761 (2015).
21. Qiu Y, Yang Y and Yang H. The unique surface molecules on intestinal intraepithelial lymphocytes: from tethering to recognizing. *Dig. Dis. Sci.* **59**, 520-529. doi: 10.1007/s10620-013-2933-1. Epub 2013 Nov 19 (2014).
22. Godfrey, D. I., Koay, H. F., McCluskey, J. & Gherardin, N. A. The biology and functional importance of MAIT cells. *Nat Immunol* **20**, 1110-1128, doi:10.1038/s41590-019-0444-8 (2019).

23. Tomura, M. *et al.* Activated regulatory T cells are the major T cell type emigrating from the skin during a cutaneous immune response in mice. *J. Clin. Invest.* **120**, 883-893, doi:10.1172/JCI40926 (2010).
24. Mazzini, E., Massimiliano, L., Penna, G. & Rescigno, M. Oral tolerance can be established via gap junction transfer of fed antigens from CX3CR1+ macrophages to CD103+ dendritic cells. *Immunity* **40**, 248-261, doi:10.1016/j.immuni.2013.12.012 (2014).
25. Eberl, G. & Littman, D. R. Thymic origin of intestinal alphabeta T cells revealed by fate mapping of RORgammat+ cells. *Science* **305**, 248-251, doi:10.1126/science.1096472 (2004).
26. Manjunath N1, von Andrian UH. *et al.* A transgenic mouse model to analyze CD8(+) effector T cell differentiation in vivo. *Proc. Natl. Acad. Sci. U S A* **96**, 13932-13937 (1999).
27. Iparraguirre, A. *et al.* Two distinct activation states of plasmacytoid dendritic cells induced by influenza virus and CpG 1826 oligonucleotide. *J. Leukoc. Biol.* **83**, 610-620, doi:10.1189/jlb.0807511 (2008).
28. Abtin, A. *et al.* Perivascular macrophages mediate neutrophil recruitment during bacterial skin infection. *Nat. Immunol.* **15**, 45-53, doi:10.1038/ni.2769 (2014).
29. Klose, C. S. et al. The transcription factor T-bet is induced by IL-15 and thymic agonist selection and controls CD8αα(+) intraepithelial lymphocyte development. *Immunity* **41**, 230-243, doi:10.1016/j.immuni.2014.06.018 (2014).
30. Konkel, J. E. et al. Control of the development of CD8αα+ intestinal intraepithelial lymphocytes by TGF-β. *Nat Immunol* **12**, 312-319, doi:10.1038/ni.1997 (2011).
31. Madakamutil, L. T. et al. CD8alphaalpha-mediated survival and differentiation of CD8 memory T cell precursors. Science 304, 590-593, doi:10.1126/science.1092316 (2004).
32. Van Kaer, L., Rabacal, W. A., Scott Algood, H. M., Parekh, V. V. & Olivares-Villagómez, D. In vitro induction of regulatory CD4+CD8α+ T cells by TGF-β, IL-7 and IFN-γ. PLoS One 8, e67821, doi:10.1371/journal.pone.0067821 (2013).

33. Mou, Z. et al. MHC class II restricted innate-like double negative T cells contribute to optimal primary and secondary immunity to Leishmania major. *PLoS Pathog* **10**, e1004396, doi:10.1371/journal.ppat.1004396 (2014).

Supplementary information is available in the online version of the paper.

Acknowledgements We thank Y. S. Yang and S. Omid for technical support; L. Jones, E. Nigro, G. Cheng and T Arai for secretarial assistance; Dr. M. Tomura for providing Kaede-tg mice; Dr. M. Bose for providing MHC-II-eGFP mice; Dr. H. Tezuka and K. Nozaki for providing the protocol for IEL separation; Dr. K. Furuhashi for providing the design of in vivo imaging device; all members of the von Andrian Lab in MHS (Especially, A. Thiriot, H. Takamatsu, S. Stutte, D. Alvarez, J. Ordovas, S. Rakoff-Nahoum, S. Loughhead, C. Gerlach, I. Mazo, M. Perro, G. Stary, R. Gonzalez and O. Barreiro) and M. Watanabe Lab in TMDU for discussion and advice. This work was supported by National Institutes of Health (NIH) grants: AI112521 and AR068383, JSPS KAKENHI grants; 17K09371, 16K09391, 19K08437, 19H03634 and 19H01050, AMED (Japan Agency for Medical Research and Development) grant; 19bm0404055h0001, 19bm0304001h0007 and 19bk0104008h0002, The Uehara Memorial Foundation grant, Astellas Foundation for Research on Metabolic Disorders grant, Mochida Memorial Foundation for Medical and Pharmaceutical Research grant and Naoki Tsuchida Research Grant.

Author Contributions Y.N., M. W., and U.H.v.A. designed the study. Y. N., S. T., Y. T. and R. M. performed and collected data from experiments, and S. O., T. N., R. O., K. T. and T. N. gave conceptual advice. K. T. and K. O. helped to collect human samples. C. X., and H. O. contributed to experiments in Figure 3b-h and provided technical support. Y. N. wrote the manuscript.

Author Information Reprints and permissions information is available at www.nature.com/reprints. The authors declare no competing financial interests. Readers are welcome to comment on the online version of the paper. Correspondence and requests for materials should be addressed to Y. N.

(ynemoto.gast@tmd.ac.jp).

Figure Legends.

Figure 1

DNT cells express high level of MHC class II and low level of co-stimulatory molecules and have the antigen uptake and process ability. (a) Gating strategy of each fraction. Dot plot is representative one of small intestinal IELs. **(b)** Difference in MHC-II expression between young 6 weeks-old mice and old 10 weeks-old mice. We repeated more than 3 independent experiments and total n=6 in this experiment. Graph shows mean + S.E.M. *P<0.05, N.S. means no significant difference. **(c)** Relationship between % of MHC-II$^+$ cells in LP DNT cells and Animal Age of a series of independent experiments with various ages. Total n=25. “r” shows Pearson product-moment correlation coefficient and P=0.278 x 10^{-4}. **(d)** Expression of MHC-II on each fraction in each organ. Dot plot is representative one. The number on each dot plot shows the mean percentage of MHC-II$^+$ cells. We repeated more than 3 independent experiments and total n=12 in this experiment. **(e)** Expression of CD80, CD86 and CD40 on each fraction. Histogram is the representative one. The number on each plot shows the mean percentage of CD80$^+$, CD86$^+$ or CD40$^+$ cells. We repeated 2 independent experiment and total n=5. **(f)** Heat map of each fraction markers and MHC-II related molecules. Result of microarray analysis of sort purified γδ, DN, CD4 and CD8 T cells. Expression values shows log2 of signals after global normalization. **(g)** Antigens uptake ability of each fraction of IELs. Histogram is the representative one. The number on each plot shows the mean percentage of DQ-OVA$^+$ cells. Graph shows mean + S. E. M. *P<0.05. We repeated more than 4 independent experiments and total n=8.

Figure 2

DNT cells uptake soluble Ags *in vivo*, migrate to MLN and present Ags to naïve CD4$^+$ T cells. (a) Percentage of MHC-II$^+$ Dextran-Alexa Flour 488$^+$ cells in each organ was analyzed 5 hours after injection of Dextran-Alexa Flour 488 into ligated small intestine. Dot plots are representative of at least 5 independent experiments and totally 8 mice were analyzed. **(b)** Representative dot plot of

Kaede-red and Kaede-green expression of photo-converted of non-converted cells. **(c)** Percentage of photo-converted cells in IEL, MLN and SP of Kaede-Tg mice 0 or 48 hours after laser irradiation. We repeated 2 independent experiments and totally 6 mice were analyzed. Graph shows mean + S.E.M. *P<0.05. ***

(d-g) Sort purified γδ, DN, CD4 or CD8 T cells in PP or $CD11c^+$ cells in MLN were co-cultured with CFSE-labeled OTII-$CD4^+$ T cells and full-length OVA. On day 5, 6 and 8, incorporation of CFSE and the number of recovered OTII-$CD4^+$ T cells were checked. We repeated 4 independent experiments and total n=6. **(d)** CFSE in corporation of OTII-$CD4^+$ T cells co-cultured with each subset on day 5, day 6 and day 8. Histogram shows representative one. **(e)** The number of recovered OT-II $CD4^+$ T cells. Graph shows mean ± S. E. M. *P<0.05. **(f)** According to the number of cell division, recovered OTII-$CD4^+$ T cells could be classified as 1 to 7^{th} generation (1^{st} generation should be undivided cells). Graph shows the percentage of each generation in OTII-$CD4^+$ T cells co-cultured with γδ, DN or CD11c on day 5, 6 and 8. Graph shows mean ± S. E. M. **(g)** Density of Th1 cytokines in the culture supernatant of each subset on day 5. Graph shows mean ± S. E. M. *P<0.05. **(h-j)** Antigen uptake/process/presentation ability of DNT cells *ex vivo*. WT mice were fed with diet including 1% OVA 3 days. Then γδ, DN, CD4, CD8 or $TCR\gamma\delta^-TCR\alpha\beta^-$ cells in PP or $CD11c^+$ cells in MLN were collected and co-incubated with CFSE-labeled OT-II $CD4^+$ T cells without exogenous OVA. Four days later, incorporation of CFSE and the number of recovered OTII-$CD4^+$ T cells were checked. We repeated 4 independent experiments and total n=8. **(h)** CFSE incorporation of OTII-$CD4^+$ T cells co-cultured with each subset. Histogram shows representative one. The number shows mean percentage of divided cells. **(i)** The number of recovered OT-II $CD4^+$ T cells. Graph shows mean ± S. E. M. *P<0.05. **(j)** Percentage of divided cells in OTII-$CD4^+$ T cells co-cultured with each subset. Graph shows mean ± S. E. M. **(k)** MHC-II dependent anergy induction ability of DNT cells. Experimental design is in **Supplemental figure 18a.** Graph shows the number of recovered OT-II $CD4^+$ T cells, mean ± S. E. M.. Black bar is the result of WT PP cells, and white bar is the result of PP cells from $CD4Cre^+$ x $H2\text{-}Ab1^{fl/fl}$ mice. We repeated more than 3 independent experiments and total n=8.

Figure 3

DNT cells extend to luminal space and take up luminal antigens. (a) In vivo live-imaging of small intestine of DPE-GFP mice. Green: GFP, blue: Hoeshct 33342, red: intra-luminal dextran-Alexa Flour 594. **(b)** In vivo live-imaging of small intestine of Tcrd-GFP mice. **(c)** In vivo live-imaging of small intestine of DPE-GFP x RAG1$^{-/-}$ mice. **(d)** In vivo live-imaging of small intestine of $CX_3CR1^{GFP/WT}$ mice. **(e)** Mean speed of all GFP$^+$ cells from 0 to 150 second in each movie was calculated by Imaris. Error bar shows mean ± S. E. M. *P<0.05. **(f)** Mean track length of all GFP$^+$ cells from 0 to 150 second in each movie was calculated by Imaris. Error bar shows mean ± S. E. M. *P<0.05**,** N.S. means no significant difference. **(g)** The number of GFP$^+$ cells contacted with IECs in representative 11 time points in each movie. Graph shows mean + S. E. M. *P<0.05. **(h)** The number of GFP$^+$ cells contacted with lumen in representative 11 time points in each movie. Graph shows mean + S. E. M. *P<0.05. **(i)** GFP$^+$ cells in DPE-GFP shapes amoeboid form and extend to LE space. **(j)** GFP$^+$ cells in DPE-GFP mice uptake luminal antigens. **(k-h)** To compare the motility of each fraction, γδ, DN, CD4, CD8$^+$ SI-IELs from EGFP-Tg mice were adoptively transferred into NSG mice. Six weeks after, in vivo live-imaging was performed. In vivo live-imaging of small intestine of γδ transferred mice **(k)**, DN transferred mice **(l)**, CD4 transferred mice **(m)** and CD8 transferred mice **(n)**. **(o)** Mean speed of all GFP$^+$ cells from 0 to 150 second in each movie was calculated by Imaris. Error bar shows mean ± S. E. M. *P<0.05. **(p)** Mean track length of all GFP$^+$ cells from 0 to 150 second in each movie was calculated by Imaris. Error bar shows mean ± S. E. M. *P<0.05**,** N.S. means no significant difference. **(q)** The number of GFP$^+$ cells contacted with IECs in representative 11 time points in each movie. Graph shows mean + S. E. M. *P<0.05. **(r)** The number of GFP$^+$ cells contacted with lumen in representative 11 time points in each movie. Graph shows mean + S. E. M. *P<0.05.

Figure 4

MHC class II$^+$ DNT cells keep the homeostasis of intestinal immune system. **(a)** Percent of initial body weight in each group. CD4-Cre$^+$ x H2-Ab1$^{flox/flox}$ mice

(KO) or age matched, sex matched littermates (WT) were given 3%DSS (DSS) or DW (DW) for 5 days, and analyzed on day 9. **(b)** Representative gross appearance of colon, MLN and SP on day 9. **(c)** Colon length of each group on day 9. **(d)** Clinical score of each group on day 9. **(e)** H&E staining of colon in each group on day 9. **(f)** Histological score of each group on day 9. Data is the representative one of 5 independent experiments includes 3-5 mice per group. **(g)** Percentage of each fraction of IEL and LPL of CD patients and non-IBD patients. Dot plot is the representative one. The number on each plot shows mean percentage of each fraction. Graph shows mean + S.E.M. *P<0.05, N.S. means no significant difference. Total n=10. **(h)** Expression of HLA-DR on each fraction of SI-LPL of CD patients and non-IBD patients. The number on each plot shows mean percentage of HLA-DR^{+} (black) or mean MFI of HLA-DR (blue). Graph shows mean + S.E.M. *P<0.05, N.S. means no significant difference. Total n=11. **(i)** Incorporation of OVA-DQ in each fraction of SI-LPL of CD patients and non-IBD patients. The number on each plot shows mean percentage of OVA-DQ^{+}. Graph shows mean + S.E.M. *P<0.05, N.S. means no significant difference. Total n=5.

Materials and Methods

Mice. C57BL/6 mice, 5-10 weeks old, were purchased from Jackson Laboratory or Charls Rriver in US and Japan CLEA in Japan. Tcrd-eGFP mice, $CX_3CR1^{GFP/WT}$ mice, RAG-1$^{-/-}$ mice, CD4-Cre mice, H2-Ab1$^{flox/flox}$ mice, CD45.1^{+}OTII x TCRα$^{-/-}$ mice and EGFP-Tg mice were purchased from Jackson Laboratory. NOD.Cg-PrkdcscidIL2Rγ$^{-/-}$ mice (NSG mice) were purchased from Charles River Japan.

MHC-II-eGFP mice were kindly given by Dr. M. Boes. Kaede-Tg mice were kindly given by Dr. M. Tomura in Kyoto University. DPE-GFP mice were originally developed in von Andrian Lab. Both male and female mice were used for experiments. All mice were intercrossed and maintained under the specific pathogen-free conditions in the Animal Care Facility of the department of microbiology and immunobiology (MBIB), Harvard Medical School or Center for Experimental Animals in Tokyo Medical and Dental University (TMDU). All experiments were approved by the animal study committees and were performed

according to institutional guidelines and Home Office regulations.

Antibodies. For mice, following antibodies were used, anti-mouse CD3e-FITC, -PerCP-Cy5.5, -Alexa Flour 647 or -APC-Cy7 (clone 145-2C11; BioLegend), CD4-PE, -APC, –PE-Cy7 or -Brilliant Violet 510 (clone RM4-5; BioLegend), anti-mouse CD5-PerCP-Cy5.5 (clone 53-7.3; BioLegend), anti-mouse CD8α-Brilliant Violet 421 (clone 53-6.7; BioLegend), anti-mouse CD8β-PE or –PerCP-Cy5.5 (clone YTS156.7.7; BioLegend), anti-mouse CD11c-PE (clone N418; BioLegend), anti-mouse CD11c-APC (clone HL3; BD Pharmingen), anti-mouse CD25-PE or –Brilliant Violet 510 (clone PC61; BioLegend), anti-mouse CD40-Alexa Flour 488 (clone HM40-3; BioLegend), anti-mouse CD44-APC (clone IM7; BioLegend), anti-mouse CD45-PE-Cy7 (clone 30-F11; BioLegend), anti-mouse CD45.1-APC or PE-Cy7 (clone A20; BioLegend), anti-mouse CD62L-FITC or -APC-Cy7 (clone MEL-14; BioLegend), anti-mouse CD69-Brilliant Violet 421 (clone H1.2F3; BioLegend), anti-mouse CD80-Brilliant Violet 421 (clone 16-10A1; BioLegend), anti-mouse CD86-Brilliant Violet 510 (clone GL-1; BioLegend), anti-mouse TCRβ-PE, APC-Cy7 or –Pacific Blue (clone H57-597; BioLegend), anti-mouse γδTCR-APC or -PE-Cy7 (clone GL3; BioLegend), anti-mouse TCRVα2-PE or -APC-Cy7(clone B20.1; BioLegend), anti-mouse MHC-II-FITC (clone M5/114.15.2; eBioscience), anti-mouse MHC-II-APC-Cy7 (clone M5/114.15.2; BioLegend), anti-mouse B220-APC-Cy7 (clone RA3-6B2; BioLegend), anti-mouse EpCAM-APC (clone G8.8; BioLegend), anti-mouse NK1.1-APC-Cy7 (clone PK136; BioLegend), anti-mouse IFN-γ-FITC (clone XMG1.2; BD Pharmingen) and anti-mouse IL-17A-PE (clone TC11-18-H10; BD Pharmingen), anti-mouse Foxp3-Alexa Flour 488 or -APC (clone FJK-16s; eBioscience) and anti-mouse RORγt-APC (clone B2D; eBioscience)
For human, following antibodies were used, anti-human CD3-FITC or-Pacific Blue (HIT3a; BioLegend), anti-human CD4-APC-Cy7 (RPA-T4; BioLegend), anti-human CD8β-eFlour 660 (SIDI8BEE; eBioscience), anti-human TCRαβ-PE-Cy7 (IP26; BioLegend), anti-human TCRγδ-PE or- PerCPCy5.5 (B1; BioLegend) and anti-human HLA-DR-PE (LN3; eBioscience).

Isolation of mononuclear cells from murine organs. To isolate SP, MLN and

PP cells, each organ was mashed and filtrated with the nylon mesh. To lyse red blood cells in splenocytes, Ack buffer was used. To isolate small intestinal-IELs or LPLs, we used the modified protocol of the previous reports[1, 2]. A half-length of distal ileum, proximal ileum, distal jejunum and proximal jejunum was opened longitudinally, washed with Hanks' balanced salt solution (HBSS) medium, and cut into small pieces. The dissected mucosae were gently inverted (50-60rpm) with the rotator for 10-15 min at 37℃ with 40ml of HBSS medium containing 2mM EDTA. Then supernatant and remaining mucosae were separated with the nylon mesh. Supernatant was centrifuged and re-suspended with 40% isotonic Percoll (GE Healthcare) solution and then subjected to Ficoll–Hypaque density gradient centrifugation (40%/75%). Collected cells were lELs. Remaining mucosae were gently inverted (50-60rpm) with rotator for 15-20 min at 37℃ with 40ml of HBSS medium containing 0.5mg/ml collagenase D (Roche) and 25μg/ml DNaseI (Roche). Then they were filtrated, centrifuged and separated with percoll system as mentioned above. To isolate colonic IELs and LPLs, the same method was used, but incubation time for EDTA and digestion was 60 min.

Flow cytometry analysis and cell sorting. To stain surface molecules, the single-cell suspension isolated from each organ was incubated with specific antibodies for 20 min at 4°C. For analysis, cells were re-suspended with PBS and acquired with FACS Canto (BD Bioscience) or FACS Canto II (BD Bioscience). To stain intracellular molecules, such as RORγt, surface molecules were stained as described above, cells were fixed with Foxp3 staining kit (eBioscience), then washed and stained with anit-RORγt antibody, according to the manufacturer's recommendation. Data was analyzed with FlowJo software (FlOWJO LLC). For cell sorting, stained cells were sorted using FACS Aria (BD Bioscience), FACS Melody (BD Bioscience) or MofloXDP (BECKMAN COULTER). Cell sorting was performed in MBIB Flow core in HMS, FACS Core Laboratory in Center for Stem Cell Biology and Regenerative Medicine in The Institute of Medical Science The University of Tokyo (IMSUT), Stem Cell Laboratory in Medical Research Institute in TMDU or Center for Stem Cell and Regenerative Medicine in TMDU. Before the each cell sorting, 7-AAD (BioLegend) staining method was used for dead cell removal. After the each cell sorting, more than 98% purity of each fraction was

confirmed by post-sort purity check with FACS Canto.

Intracellular staining of cytokines. Small intestinal IELs (SI-IEL) were collected from 6-10 weeks old C57BL/6 mice and stained with anti-mouse CD8β-PerCP-Cy5.5, anti-mouse CD4-APC-Cy7, anti-mouse TCRβ-Pacific Blue and anti-mouse γδTCR-PE-Cy7, and then sorted with FACS Aria as following fractions, $\gamma\delta TCR^{+}TCR\beta^{-}$ (γδ), $\gamma\delta TCR^{-}TCR\beta^{+}CD4^{-}CD8\beta^{-}$ (DN), $\gamma\delta TCR^{-}TCR\beta^{+}CD4^{+}CD8\beta$ (CD4) and $\gamma\delta TCR^{-}TCR\beta^{+}CD4^{-}CD8\beta^{+}$ (CD8). We confirmed more than 98% purity of each fraction by analyzing post-sorted cells with FACS Canto. Sorted cells were cultured for 6 hours with ionomycine (500 ng/ml), PMA (20ng/ml) and BD GolgiPlug (1μl/ml BD Pharmingen). Following cell fixation using a Foxp3 staining kit (eBioscience), the cells were incubated with anti-IL-17A-PE and anti-IFN-γ-FITC for 20 min. Then cells were washed and analyzed with FACS Canto.

Microarray Analysis. PP cells were collected from 10 weeks old C57BL/6 mice and were stained with anti-CD8β-PE, anti-CD4-APC, anti-TCRβ-APC-Cy7 and anti-γδTCR-PE-Cy7, then sorted with MofFlo-XDP as following fractions, $\gamma\delta TCR^{+}TCR\beta^{-}$ (γδ), $\gamma\delta TCR^{-}TCR\beta^{+}CD4^{-}CD8\beta^{-}$ (DN), $\gamma\delta TCR^{-}TCR\beta^{+}CD4^{+}CD8\beta$ (CD4) and $\gamma\delta TCR^{-}TCR\beta^{+}CD4^{-}CD8\beta^{+}$ (CD8). We confirmed more than 98% purity of each fraction analyzing post-sorted cells with FACS Canto II. Whole mRNA was collected from each fraction with RNeasy Mini Kit (QIAGEN). Microarray analysis was outsourced to KAMAKURA TECHNO-SCIENCE INC. Samples were analyzed with the 3D gene chip (Mouse oligo 24k).

***In vitro* uptake of DQ-OVA and pHrodo green E. coli.** SI-IELs were collected from 6-10 weeks old C57BL/6 mice and stained with anti-CD8β-PE, anti-CD4-APC, anti-TCRβ-APC-Cy7 and anti-γδTCR-PE-Cy7, then sorted with FACS Aria or MofFlo-XDP as following fractions: $\gamma\delta TCR^{+}TCR\beta^{-}$ (γδ), $\gamma\delta TCR^{-}TCR\beta^{+}CD4^{-}CD8\beta^{-}$ (DN), $\gamma\delta TCR^{-}TCR\beta^{+}CD4^{+}CD8\beta$ (CD4) and $\gamma\delta TCR^{-}TCR\beta^{+}CD4^{-}CD8\beta^{+}$ (CD8). Murine MLN cells were stained with anti-CD11c-PE, anti-TCRβ-APC-Cy7 and anti-γδTCR-PE-Cy7, sorted as $\gamma\delta TCR^{-}TCR\beta^{-}CD11c^{+}$ (CD11c). 1×10^{5} cells of each fraction was co-incubated with or without 20μg/ml DQ-OVA in RPMI medium with 10% FBS, HEPES and 2ME in the condition of 37℃ and 5%CO_2. 1

x 10^5 of each fraction was also incubated with pHrodo green E. coli according to the manufacturer's instructions. Five hours later, cells were collected and analyzed by FACS.

***In vivo* uptake of Dextran-AF488.** A small incision was made on the abdomen of anesthetized C57BL/6 mice, and then small intestine was exposed and ligated for 5cm long. 500μg of 10KDa Dextran-Alexa Flour 488 (Molecular Probes) was injected in a volume of 100μl into the ligated loop. Five hours later, mice were euthanized and cells in SI-IEL, SI-LPL, PP, MLN and SP were isolated, stained with anti-CD4-PE, CD8β-PerCP-Cy5.5, γδ-TCR-APC, TCRβ-PE-Cy7 and MHC-II-APC-Cy7. Then incorporation of dextran-AF488 in each fraction was analyzed with FACS Canto.

Photoconversion experiment with Kaede-Tg mice. We used modified protocol of the previous reports[3,4]. A small incision was made on the abdomen of anesthetized mice, and then small intestine was exposed. Avoiding Peyer's patches, vessels and other organs, 3cm of small intestine was irradiated with violet light laser (Electra Pro Series 405nm Violet Portable Laser, Laserglow Technologies) from serosal side for 5 min. Forty-eight hours later, mice were euthanized and cells in SI-IEL, SI-LPL, PP, MLN and SP were isolated, stained with anti-CD8β-PerCP-Cy5.5, γδ-TCR-APC, TCRβ-PE-Cy7 and CD4-APC-Cy7. Then percentage of converted-Kaede and inconverted-kaede in each fraction was analyzed with FACS Canto II.

***In vitro* antigen presentation.** PP cells were collected from 6-8 weeks old C57BL/6 mice and stained with anti-CD8β-PE, anti-CD4-APC, anti-TCRβ-APC-Cy7 and anti-γδTCR-PE-Cy7, then sorted out as following fractions, $\gamma\delta TCR^+TCR\beta^-$ (γδ), $\gamma\delta TCR^-TCR\beta^+CD4^-CD8\beta^-$ (DN), $\gamma\delta TCR^-TCR\beta^+CD4^+CD8\beta^-$ (CD4) and $\gamma\delta TCR^-TCR\beta^+CD4^-CD8\beta^+$ (CD8) and $\gamma\delta TCR^-TCR\beta^-$ (TCR-). In some experiment, same fraction in SI-IEL, SI-LPL or MLN was also used. MLN cells from C57BL/6 mice were stained with anti-CD11c-PE, anti-TCRβ-APC-Cy7 and anti-γδTCR-PE-Cy7, sorted as $\gamma\delta TCR^-TCR\beta^-CD11c^+$ (CD11c). Cells were collected from SP and MLN of $CD45.1^+$ OTII-Tg mice and stained with CD62L-

FITC, TCRVα2-PE, CD44-APC and CD4-PE-Cy7 and sorted as $CD4^+TCRV\alpha2^+CD44^-CD62L^+$ (OTII $CD4^+$). 1 x 10^4 of each fraction was co-incubated with or without 100μg of Ovalbumin (Low-endotoxin grade, Wako, Japan) and 1 x 10^5 of CFSE labeled OTII $CD4^+$ T cells in PRMI medium with 10% FBS, HEPES and 2ME in the condition of 37℃ and 5%CO_2. On day 5, 6 and 8, after the collection of supernatant and cell count, recovered cells were washed and stained with anti-mouse CD44-APC, CD45.1-PE-Cy7, CD62L-APC-Cy7 CD69-brilliant violet 421, CD25-brilliant violet 510 and 7-AAD, and fluorescent of CFSE on $7AAD^-CD45.1^+$ cells was analyzed with FACS. As a negative control, we confirmed that no cell division occurs in the wells of 1x 10^5 OTII CD4 and OVA. Cytokine Bead Assay (CBA) was performed with supernatant using mouse Th1/Th2/Th17 Cytokine Kit and FCAP Array™ Software version 3.0.

***Ex vivo* antigen presentation.** First, 8-10 weeks old WT mice (C57BL/6J, Japan CLEA) were fed with diet (powder type normal diet CE-2, Japan CLEA) including 1%(w/w) ovalbumin (Nakarai, Japan) for 3 days. Then γδ, DN, CD4, CD8 or $TCR\gamma\delta^-TCR\alpha\beta^-$ cells in PP or $CD11c^+$ cells in MLN were collected and 1 x 10^4 of them were co-incubated with 1 x 10^5 CFSE-labeled (2.5μM) OT-II $CD4^+$ T cells without exogenous ovalbumin. Four days later, incorporation of CFSE and the number of recovered $7AAD^-Ly5.1^+CD4^+$ cells (OTII-$CD4^+$ T cells) were checked. Staining pattern and definition of each fraction are same as *in vitro* antigen presentation experiment.

***In vitro* anergy induction.** PP cells were collected from 8-10 weeks old $CD4Cre^+$ x $H2\text{-}Ab1^{fl/fl}$ mice or age and sex matched WT mice and stained with anti-CD8β-PE, anti-CD4-APC, anti-TCRβ-APC-Cy7 and anti-γδTCR-PE-Cy7, then sorted out with FACS Aria as following fractions, $\gamma\delta TCR^+TCR\beta^-$ (γδ), $\gamma\delta TCR^-TCR\beta^+CD4^-CD8\beta^-$ (DN), $\gamma\delta TCR^-TCR\beta^+CD4^+CD8\beta^-$ (CD4) and $\gamma\delta TCR^-TCR\beta^+CD4^-CD8\beta^+$ (CD8). MLN cells from C57BL/6 mice were stained with anti-CD11c-PE, anti-TCRβ-APC-Cy7 and anti-γδTCR-PE-Cy7, sorted as $\gamma\delta TCR^-TCR\beta^-CD11c^+$ (CD11c). Cells were collected from SP and MLN of $CD45.1^+$ OTII-Tg mice and stained with CD62L-FITC, CD44-APC, CD4-PE-Cy7 and TCRVα2-PE and sorted as $CD4^+TCRV\alpha2^+CD44^-CD62L^+$ cells (OTII $CD4^+$). First, 1 x 10^4

of γδ, DN, CD4 or CD8 cells from PP were co-incubated with 1μg of $OVA_{323-329}$ and 1 x 10^5 of CFSE labeled OTII $CD4^+$ T cells. Two hours later, 1 x 10^4 $CD11c^+$ cells were added into each well. Cells were incubated in PRMI medium with 10% FBS, HEPES and 2ME in the condition of 37℃ and 5%CO_2. Four days later, cells were collected, washed and stained with anti-mouse CD4-PE-Cy7, anti-mouse CD45.1-APC and 7-AAD, and fluorescent of CFSE on $7AAD^-CD4^+CD45.1^+$ cells was analyzed with FACS Canto. As a positive control, we prepared wells of 1x 10^4 $CD11c^+$, 1x 10^5 OTII CD4 and 1μg $OVA_{323-329}$. As a negative control, we confirmed that no cell division occurs in the wells of 1x 10^5 OTII CD4 and 1μg $OVA_{323-329}$.

***In vivo* live imaging.** Mice were anesthetized and injected intravenously with Hoechst 33342 dye (sigma). A small incision was made on the abdomen and small intestine was exposed. Then mice were fixed on the customized stage for in vivo live imaging and temperature of core and exposed small intestine was maintained at 37℃ with the heating plate. Small intestine was gently opened along the antimesenteric border. 10K Dalton Dextran Alexa Flour 594 (Molecular Probes) was added on the luminal side and coverslip was put on it. Cell behavior was recorded for 10-60 min. In HMS, in vivo imaging was performed using the two-photon microscope with the x20 water-immersion objective of an upright microscope (Prairie Technologies). A MaiTai Ti:sapphire laser (Spectra-Physics) was tuned between 870 nm and 900 nm for multiphoton excitation. In TMDU, in vivo imaging was performed using the FV1200MPE (Olympus) in Dr. Okazawa Lab or A1RMP (Nikon) in Watanabe Lab. For dynamic analysis of cell movement, several x–y sections (512 x 512) were acquired every 2–30s. Emitted light and second-harmonic signals were directed through 450/80 nm, 525/50 nm and 630/120 nm bandpass filters and detected with non- descanned detectors. Post-acquisition image analysis and time-lapse videos were performed using Imaris software (Bitplane scientific software).

Adoptive transfer experiment. IELs were collected from small intestine of EGFP-Tg mice. Then stained with anti-CD8β-PerCP-Cy5.5, anti-CD4-APC, anti-TCRγδ-PE-Cy7 and anti-TCRβ-APC-Cy7, then sorted out with FACS Aria as

following fractions, γδTCR^{+}TCRβ^{-} (γδ), γδTCR^{-}TCRβ^{+}CD4^{-}CD8β^{-} (DN), γδTCR^{-}TCRβ^{+}CD4^{+}CD8β^{-} (CD4) and γδTCR^{-}TCRβ^{+}CD4^{-}CD8β^{+} (CD8). 5 x 10^{5} cells of each fraction were re-suspended with PBS and transferred into NSG mice (6 weeks-old, female) by intraperitoeal administration. Seven to eight weeks later, in vivo live-imaging of each mouse was performed.

DSS colitis model. CD4Cre^{+} x H2-Ab1$^{fl/fl}$ mice and age matched, sex matched littermates in the same cage were assigned as each group. Then, 3% (wt/vol) 36-50KDa dextran sulfate (DSS, MP Biochemicals, LLC) solution is administered as drinking water for 5 days. The remaining DSS solution was replaced by autoclaved water on day 6. The condition and the body weights of mice were checked every day during and several days after the DSS administration. Mice were sacrificed and analyzed on day 9. At autopsy, their clinical scores were assessed as the sum of three parameters: hunching and wasting, 0 or 1; colon thickening, 0–3 (0, none; 1, mild; 2, moderate; or 3, extensive); and stool consistency, 0–3 (0, normal beaded stool; 1, soft stool; 2, diarrhea; 3, bloody stool)[5]. Tissue samples were fixed in PBS containing 10% neutral-buffered formalin. Paraffin-embedded sections (5 μm) were stained with H&E. For histological score, the presence of occasional inflammatory cells in the lamina propria was assigned a value of 0; increased numbers of inflammatory cells in the lamina propria a value 1, confluence of inflammatory cells, extending into the submucosa a value of 2, and transmural extension of the infiltrate a value of 3. The presence of occasional inflammatory cells in the lamina propria was assigned a value of 0; increased numbers of inflammatory cells in the lamina propria a value 1, confluence of inflammatory cells, extending into the submucosa a value of 2, and transmural extension of the infiltrate a value of 3. The combined histological score ranged from 0 (no changes) to 6 (extensive cell infiltration and tissue damage) [30].

Human samples. Adult patients in the hospital of TMDU from 2015 to 2019 with informed consent of this study were involved. This research was admitted by the committee for clinical research of TMDU (#M2000-2347). Biopsy samples from ileum of CD or non-IBD patients were collected by colonoscopy or balloon

assisted small bowel endoscopy. Samples were washed with Hanks' balanced salt solution (HANCS) medium, and cut into small pieces. The dissected mucosae were gently inverted (50-60rpm) with the rotator for 30 min at 37℃ with 40ml of (HANCS) containing 2mM EDTA. Then supernatant and remaining mucosa was separated with the nylon mesh. Supernatant was centrifuged and re-suspended with 40% isotonic Percoll solution and then subjected to Ficoll–Hypaque density gradient centrifugation (40%/75%). Collected cells were IELs. Remaining mucosae were gently inverted (50-60rpm) with the rotator for 30 min at 37℃ with 40ml of (HANCS) containing collagenase D and DNaseI. Then they were filtrated, centrifuged and separated with percoll system as mentioned above. Collected cells (lamina propria mononuclear cells: LPMCs) were stained with anti-HLA-DR-PE, anti-TCRγδ-PerCP-Cy5.5, anti-CD8β-APC, anti-TCRαβ-PE-Cy7, anti-CD4-APC-Cy7 and anti-CD3-Pacific blue and expression of HLA-DR on each fraction was checked by FACS Canto II. For in vitro uptake experiments, LPMCs were incubated with or without 10μg/ml DQ-OVA in PRMI medium with 10% FBS in the condition of 37℃ and 5%CO_2. Four hours later, cells were washed, collected and stained with anti-TCRγδ-PE, 7AAD, anti-CD8β-APC, anti-TCRαβ-PE-Cy7, anti-CD4-APC-Cy7, anti-CD3-Pacific blue and fluorescent of DQ-OVA in each fraction was analyzed with FACS-Canto II.

Statistical analysis. Precise experimental numbers of animals or human samples are described in the each figure legend. All statistical analyses in this study were done with *Statcel* software except for figure 3f-g analyses, which are done with Prism (GraphPad Software). We examined the normality of the distribution of results in each group. Differences between two groups were assessed using Student's t-tests; otherwise, differences were assessed using Welch's t-test. Results are expressed as mean ± SEM. Differences were considered significant when $P < 0.05$.

Movie S1. In vivo live imaging of small intestine of DPE-GFP mice. Anesthetized DPE-GFP mice were injected with Hoechst 33342 (blue) and given luminal 10kDa dextran (red). Imaging was performed from luminal surface using the two-photon microscope. GFP^+ T cells (green) dynamically move between IE

and LP.

Movie S2. In vivo live imaging of small intestine of Tcrd-eGFP mice. Anesthetized Tcrd-eGFP mice were injected with Hoechst 33342 (blue) and given luminal 10kDa dextran (red). Imaging was performed from luminal surface using the two-photon microscope. GFP^+ T cells (green) dynamically move between IE and LP.

Movie S3. In vivo live imaging of small intestine of DPE-GFP x $RAG1^{-/-}$ mice. Since it was reported that some non-T cells, we also perform intravital microscopy of small intestine of DPE-GFP x $RAG2^{-/-}$ mice. Anesthetized DPE-GFP x $RAG1^{-/-}$ mice were injected with Hoechst 33342 (blue) and given luminal 10kDa dextran (red). GFP^+ cells (green) move slowly in LP lesion.

Movie S4. In vivo live imaging of small intestine of $CX_3CR1^{GFP/WT}$ mice. Anesthetized $CX_3CR1^{GFP/WT}$ mice were injected with Hoechst 33342 (blue) and given luminal 10kDa dextran (red). Imaging was performed from luminal surface using the two-photon microscope. Although GFP^+ cells (green) extend dendrite, their movement is small and slow.

Movie S5. Trans-epithelial movement of GFP^+ cells in DPE-GFP mice. Extension of Movie S1 and another in vivo imaging of DPE-GFP mice. GFP^+ cells (green) forms unique shape and extend dendrite through epithelial cell layer (blue) to luminal space (red).

Movie S6. Luminal antigen uptake of GFP^+ cells in DPE-GFP mice. DPE-GFP mice were injected with OVA-AF594 into small intestinal lumen. Three hours later, mice were anesthetized and injected with Hoechst 33342 (blue). Allows indicate GFP^+T cells (green) captured luminal OVA (red).

Movie S7. In vivo live-imaging of small intestine of NSG mice transferred with GFP^+γδ-IELs (γδ→NSG). Anesthetized γδ→NSG mice were injected with Hoechst 33342 (blue) and given luminal 10kDa dextran (red). Imaging was

performed from luminal surface using the two-photon microscope.

Movie S8. In vivo live-imaging of small intestine of NSG mice transferred with GFP$^+$DN-IELs (DN→NSG). Anesthetized DN→NSG mice were injected with Hoechst 33342 (blue) and given luminal 10kDa dextran (red). Imaging was performed from luminal surface using the two-photon microscope.

Movie S9. In vivo live-imaging of small intestine of NSG mice transferred with GFP$^+$CD4-IELs (CD4→NSG). Anesthetized CD4→NSG mice were injected with Hoechst 33342 (blue) and given luminal 10kDa dextran (red). Imaging was performed from luminal surface using the two-photon microscope.

Movie S10. In vivo live-imaging of small intestine of NSG mice transferred with GFP$^+$CD8-IELs (CD8→NSG). Anesthetized CD8→NSG mice were injected with Hoechst 33342 (blue) and given luminal 10kDa dextran (red). Imaging was performed from luminal surface using the two-photon microscope.

Movie S11. The large number of DNT cells contacted with luminal antigens. Additional movie of DN→NSG mice. There are a lot of GFP$^+$ cells in IE lesion of DN→NSG mice, compared to other groups. In addition, the large number of GFP$^+$ cells in DN→NSG mice contacted with luminal antigens.

Figures

Supplemental References

1. Nozaki K, Watanabe M and Nakamura T. *et al.* Co-culture with intestinal epithelial organoids allows efficient expansion and motility analysis of intraepithelial lymphocytes. *J. Gastroenterol.* **51,** 206-213. doi: 10.1007/s00535-016-1170-8. Epub 2016 Jan 22 (2016).
2. Tezuka H, Ohteki T. *et al.* Regulation of IgA production by naturally occurring TNF/iNOS-producing dendritic cells. *Nature* **448,** 929-933 (2007).
3. Onizawa, M. *et al.* Signaling pathway via TNF-alpha/NF-kappaB in intestinal epithelial cells may be directly involved in colitis-associated carcinogenesis. *Am. J. Physiol. Gastrointest. Liver. Physiol.* **296,** G850-859, doi:10.1152/ajpgi.00071.2008 (2009).
4. Tomura, M. et al. Activated regulatory T cells are the major T cell type emigrating from the skin during a cutaneous immune response in mice. *J. Clin. Invest.* **120**, 883-893, doi:10.1172/JCI40926 (2010).
5. Bromley SK, Yan S, Tomura M, Kanagawa O & Luster AD. Recirculating memory T cells are a unique subset of CD4+ T cells with a distinct phenotype and migratory pattern. *J. Immunol.* **190,** 97097-6. doi: 10.4049/jimmunol.1202805. Epub 2012 Dec 19 (2013).

Figure 1

DNT cells express high level of MHC class II and low level of co-stimulatory molecules and have the antigen uptake and process ability. (a) Gating strategy of each fraction. Dot plot is representative one of small intestinal IELs. (b) Difference in MHC-II expression between young 6 weeks-old mice and old 10

weeks-old mice. We repeated more than 3 independent experiments and total n=6 in this experiment. Graph shows mean + S.E.M. *P<0.05, N.S. means no significant difference. (c) Relationship between % of MHC-II+ cells in LP DNT cells and Animal Age of a series of independent experiments with various ages. Total n=25. “r” shows Pearson product-moment correlation coefficient and P=0.278 x 10-4. (d) Expression of MHC-II on each fraction in each organ. Dot plot is representative one. The number on each dot plot shows the mean percentage of MHC-II+ cells. We repeated more than 3 independent experiments and total n=12 in this experiment. (e) Expression of CD80, CD86 and CD40 on each fraction. Histogram is the representative one. The number on each plot shows the mean percentage of CD80+, CD86+ or CD40+ cells. We repeated 2 independent experiment and total n=5. (f) Heat map of each fraction markers and MHC-II related molecules. Result of microarray analysis of sort purified γδ, DN, CD4 and CD8 T cells. Expression values shows log2 of signals after global normalization. (g) Antigens uptake ability of each fraction of IELs. Histogram is the representative one. The number on each plot shows the mean percentage of DQ-OVA+ cells. Graph shows mean + S. E. M. *P<0.05. We repeated more than 4 independent experiments and total n=8.

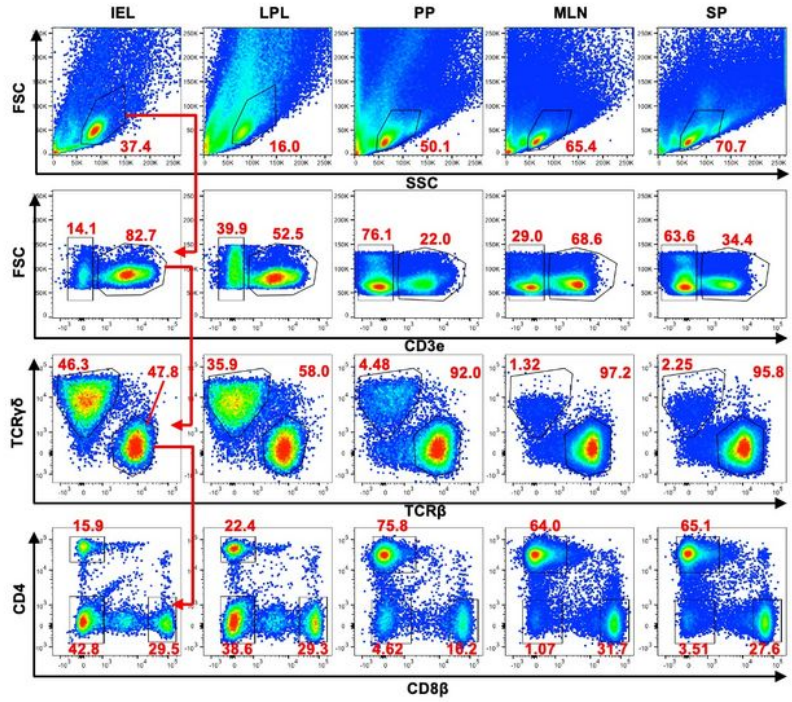

Supplemental Figure 1. Gating strategy of each fraction in each organ.
Dot plot is the representative one of the same experiments as Figure 1a and 1d. The number on each dot plot shows the mean percentage of each fraction. We repeated 3 independent experiments with 4 animals in each.

Figure 2

DNT cells uptake soluble Ags in vivo, migrate to MLN and present Ags to naïve CD4+ T cells. (a) Percentage of MHC-II+ Dextran-Alexa Flour 488+ cells in each organ was analyzed 5 hours after injection of Dextran-Alexa Flour 488 into ligated small intestine. Dot plots are representative of at least 5 independent experiments and totally 8 mice were analyzed. (b) Representative dot plot of Kaede-red and Kaede-green expression of photo-converted of non-converted cells. (c) Percentage of photo-converted

cells in IEL, MLN and SP of Kaede-Tg mice 0 or 48 hours after laser irradiation. We repeated 2 independent experiments and totally 6 mice were analyzed. Graph shows mean + S.E.M. *P<0.05. *** (d-g) Sort purified γδ, DN, CD4 or CD8 T cells in PP or CD11c+ cells in MLN were co-cultured with CFSE-labeled OTII-CD4+ T cells and full-length OVA. On day 5, 6 and 8, incorporation of CFSE and the number of recovered OTII-CD4+ T cells were checked. We repeated 4 independent experiments and total n=6. (d) CFSE in corporation of OTII-CD4+ T cells co-cultured with each subset on day 5, day 6 and day 8. Histogram shows representative one. (e) The number of recovered OT-II CD4+ T cells. Graph shows mean ± S. E. M. *P<0.05. (f) According to the number of cell division, recovered OTII-CD4+ T cells could be classified as 1 to 7th generation (1st generation should be undivided cells). Graph shows the percentage of each generation in OTII-CD4+ T cells co-cultured with γδ, DN or CD11c on day 5, 6 and 8. Graph shows mean ± S. E. M. (g) Density of Th1 cytokines in the culture supernatant of each subset on day 5. Graph shows mean ± S. E. M. *P<0.05. (h-j) Antigen uptake/process/presentation ability of DNT cells ex vivo. WT mice were fed with diet including 1% OVA 3 days. Then γδ, DN, CD4, CD8 or TCRγδ-TCRαβ- cells in PP or CD11c+ cells in MLN were collected and co-incubated with CFSE-labeled OT-II CD4+ T cells without exogenous OVA. Four days later, incorporation of CFSE and the number of recovered OTII-CD4+ T cells were checked. We repeated 4 independent experiments and total n=8. (h) CFSE incorporation of OTII-CD4+ T cells co-cultured with each subset. Histogram shows representative one. The number shows mean percentage of divided cells. (i) The number of recovered OT-II CD4+ T cells. Graph shows mean ± S. E. M. *P<0.05. (j) Percentage of divided cells in OTII-CD4+ T cells co-cultured with each subset. Graph shows mean ± S. E. M. (k) MHC-II dependent anergy induction ability of DNT cells. Experimental design is in Supplemental figure 18a. Graph shows the number of recovered OT-II CD4+ T cells, mean ± S. E. M.. Black bar is the result of WT PP cells, and white bar is the result of PP cells from CD4Cre+ x H2-Ab1fl/fl mice. We repeated more than 3 independent experiments and total n=8.

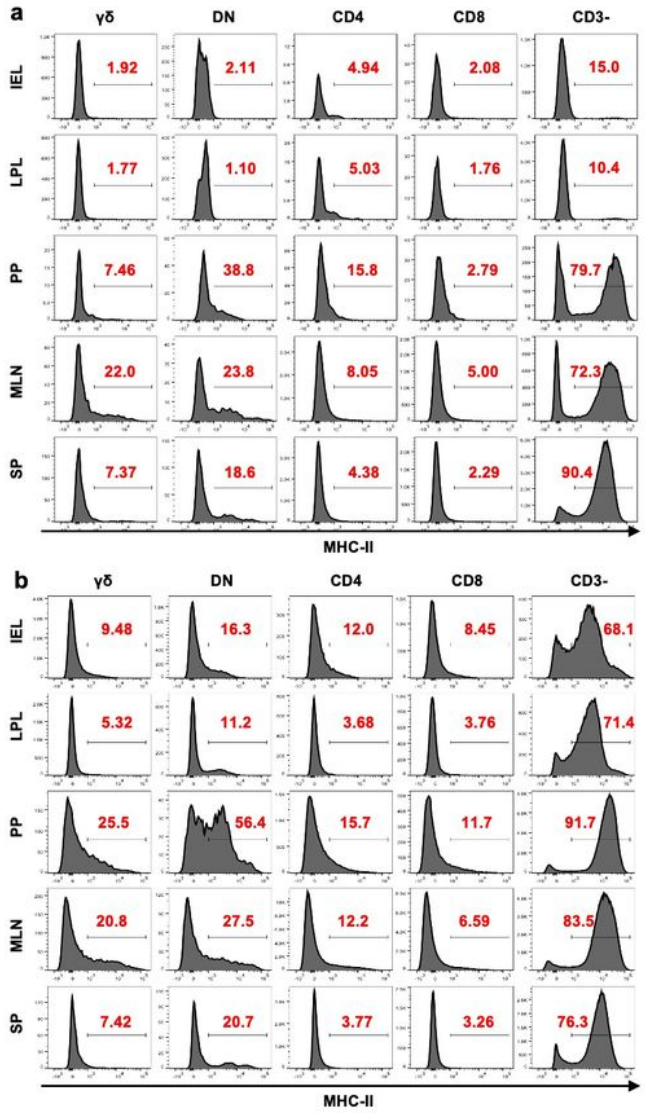

Supplemental Figure 2. Difference in expression of MHC-II on T cells between young and adult mice. (a) Flow cytometry analysis of the expression of MHC-II on γδ, DN, CD4, CD8 and CD3- cells in each organ of 6 weeks-old mice. **(b)** Flow cytometry analysis of the expression of MHC-II on γδ, DN, CD4, CD8 and CD3- cells in each organ of 10 weeks-old mice. Histograms are representative one of three independent experiments. Percentage of MHC-II$^+$ cells is shown as the mean of 6 mice per group.

Figure 3

DNT cells extend to luminal space and take up luminal antigens. (a) In vivo live-imaging of small intestine of DPE-GFP mice. Green: GFP, blue: Hoeshct 33342, red: intra-luminal dextran-Alexa Flour 594. (b) In vivo live-imaging of small intestine of Tcrd-GFP mice. (c) In vivo live-imaging of small intestine of DPE-GFP x RAG1-/- mice. (d) In vivo live-imaging of small intestine of CX3CR1GFP/WT mice. (e) Mean speed of all GFP+ cells from 0 to 150 second in each movie was calculated by Imaris. Error bar shows

mean ± S. E. M. *P<0.05. (f) Mean track length of all GFP+ cells from 0 to 150 second in each movie was calculated by Imaris. Error bar shows mean ± S. E. M. *P<0.05, N.S. means no significant difference. (g) The number of GFP+ cells contacted with IECs in representative 11 time points in each movie. Graph shows mean + S. E. M. *P<0.05. (h) The number of GFP+ cells contacted with lumen in representative 11 time points in each movie. Graph shows mean + S. E. M. *P<0.05. (i) GFP+ cells in DPE-GFP shapes amoeboid form and extend to LE space. (j) GFP+ cells in DPE-GFP mice uptake luminal antigens. (k-h) To compare the motility of each fraction, γδ, DN, CD4, CD8+ SI-IELs from EGFP-Tg mice were adoptively transferred into NSG mice. Six weeks after, in vivo live-imaging was performed. In vivo live-imaging of small intestine of γδ transferred mice (k), DN transferred mice (l), CD4 transferred mice (m) and CD8 transferred mice (n). (o) Mean speed of all GFP+ cells from 0 to 150 second in each movie was calculated by Imaris. Error bar shows mean ± S. E. M. *P<0.05. (p) Mean track length of all GFP+ cells from 0 to 150 second in each movie was calculated by Imaris. Error bar shows mean ± S. E. M. *P<0.05, N.S. means no significant difference. (q) The number of GFP+ cells contacted with IECs in representative 11 time points in each movie. Graph shows mean + S. E. M. *P<0.05. (r) The number of GFP+ cells contacted with lumen in representative 11 time points in each movie. Graph shows mean + S. E. M. *P<0.05.

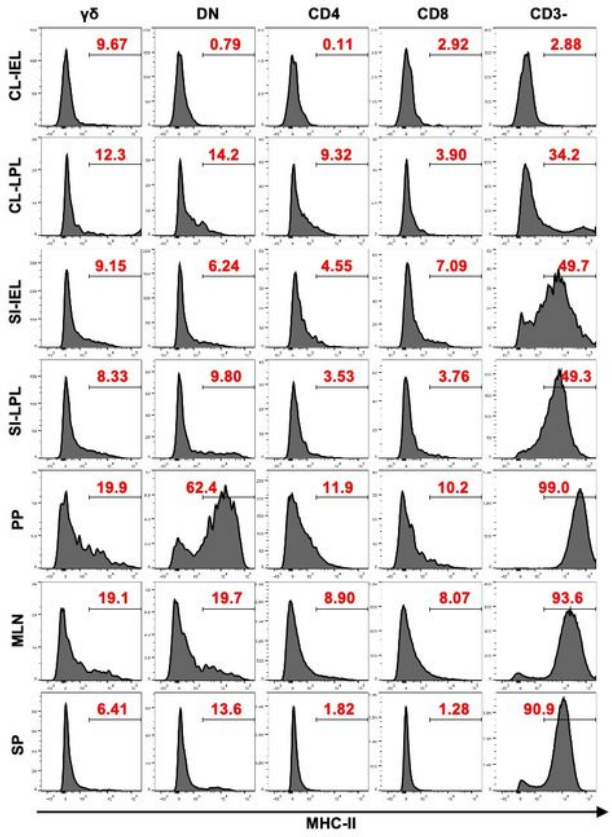

Supplemental Figure 3. γδT cells and DNT cells in colonic LP, but not colonic IEL expressed low level of MHC class II. Percentage of MHC-II$^+$ cells on γδ, DN, CD4 and CD8 T cells in colonic IEL and LPL was checked by flow cytometer. As controls, SI-IEL, SI-LPL, PP, MLN and SP were also checked. MHC-II, CD3e, TCRγδ, TCRβ, CD4 and CD8β were stained at the same time. Data are accumulation of 2 independent experiments and total n=6. Histogram is the representative one and number shows mean.

Figure 4

MHC class II+ DNT cells keep the homeostasis of intestinal immune system. (a) Percent of initial body weight in each group. CD4-Cre+ x H2-Ab1flox/flox mice (KO) or age matched, sex matched littermates (WT) were given 3%DSS (DSS) or DW (DW) for 5 days, and analyzed on day 9. (b) Representative gross appearance of colon, MLN and SP on day 9. (c) Colon length of each group on day 9. (d) Clinical score of each group on day 9. (e) H&E staining of colon in each group on day 9. (f) Histological score of each

group on day 9. Data is the representative one of 5 independent experiments includes 3-5 mice per group. (g) Percentage of each fraction of IEL and LPL of CD patients and non-IBD patients. Dot plot is the representative one. The number on each plot shows mean percentage of each fraction. Graph shows mean + S.E.M. *P<0.05, N.S. means no significant difference. Total n=10. (h) Expression of HLA-DR on each fraction of SI-LPL of CD patients and non-IBD patients. The number on each plot shows mean percentage of HLA-DR+ (black) or mean MFI of HLA-DR (blue). Graph shows mean + S.E.M. *P<0.05, N.S. means no significant difference. Total n=11. (i) Incorporation of OVA-DQ in each fraction of SI-LPL of CD patients and non- IBD patients. The number on each plot shows mean percentage of OVA-DQ+. Graph shows mean + S.E.M. *P<0.05, N.S. means no significant difference. To

Supplementary Files

This is a list of supplementary files associated with this preprint. Click to download.

- SupplementMovie1.mov
- SupplementMovie2.mov
- SupplementMovie3.mov
- SupplementMovie4.mov
- SupplementMovie5.mov
- SupplementMovie6.mov
- SupplementMovie7.mov
- SupplementMovie8.mov
- SupplementMovie9.mov
- SupplementMovie10.mov
- SupplementMovie11.mov
- XXXXXXXXXXXXXXX21.jpg
- XXXXXXXXXXXXXXX22.jpg
- supplement14.jpg
- supplement15.jpg
- supplement16.jpg
- supplement17.jpg
- XXXXXXXXXXXXXXX5.jpg
- XXXXXXXXXXXXXXX6.jpg
- XXXXXXXXXXXXXXX7.jpg
- XXXXXXXXXXXXXXX8.jpg
- XXXXXXXXXXXXXXX9.jpg

- XXXXXXXXXXXXXXX10.jpg
- XXXXXXXXXXXXXXX11.jpg
- XXXXXXXXXXXXXXX12.jpg
- XXXXXXXXXXXXXXX13.jpg
- XXXXXXXXXXXXXXX14.jpg
- XXXXXXXXXXXXXXX15.jpg
- XXXXXXXXXXXXXXX16.jpg
- XXXXXXXXXXXXXXX17.jpg
- XXXXXXXXXXXXXXX18.jpg
- XXXXXXXXXXXXXXX19.jpg
- XXXXXXXXXXXXXXX20.jpg
- XXXXXXXXXXXXXXX23.jpg
- XXXXXXXXXXXXXXX24.jpg
- XXXXXXXXXXXXXXX25.jpg